

Polymer Nanofibrous and Their Application for Batteries



Ahmed Ali Nada

Abstract Rechargeable batteries have been rapidly developed to meet the continuous demand for pursuing sustainable and renewable energy resources in order to reduce the fossil fuel consumption and CO₂ emission. In such batteries, electric energy is produced via reduction–oxidation reactions between two electrodes and electrolyte. In order to obtain such batteries with higher energy and power densities, nanoscaled functional electrodes have been an approach. In this review, electrospinning basics and challenges to develop bead-free and smooth electrospun fiber are briefly provided. Advanced techniques to produce functional electrospun fibers such as coaxial and emulsion electrospinning are described. Basics of voltaic cells were extensively illustrated by highlighting the role of each component in the cell. Differences between primary and secondary cells are explained. Applications of such functional nanofibers in the battery electrodes and electrolytes to enhance the overall performance are discussed. The discussion was focused on Metal-ion and metal–air batteries including the rule of the electrospun substrates on enhancing anodes, cathodes, and electrolytes performances. Electrochemical characteristics in terms of ionic conductivity, battery density, and capacity were highlighted. The add-on value in the performance of such advanced nanofibers in metal–air and metal-ion batteries is broadly highlighted.

Keywords Energy storage · Rechargeable batteries · Metal–air batteries · Metal-ion batteries · Power density

A. A. Nada (✉)

Pre-treatment and Finishing of Cellulosic Textiles Dept., Textile Research Division, National Research Centre (Scopus Affiliation ID 60014618), Dokki, Giza, Egypt
e-mail: aanada@ncsu.edu

Centre for Advanced Materials Application, Slovak Academy of Sciences, Dúbravská cesta 9, 845 11 Bratislava, Slovakia

1 Introduction

1.1 Basics of Battery Electrochemistry

It has been a long time for climate activists calling for effective, efficient, and clean alternative energy sources to fossil fuel with limited carbon dioxide emission to save the planet earth [1, 2]. Concurrently, many scientists have been working globally on developing alternative clean energy resources such as wind energy [3, 4], solar energy [5, 6], and biogas energy [7, 8], etc. Such different sustainable resources of energy require energy storage systems. Basically, dry cells that have been developed since the 1880s are considered as a turning point for storing electricity and operating portable electronic devices [9]. Dry cells have been divided into primary (non-rechargeable) cells and secondary (rechargeable) cells. Both cell types follow the same operating mechanism by converting chemical energy to electric energy [10, 11]. However, rechargeable cells can convert back electricity to chemical energy as well [12].

Simply, electricity can be generated when electrons move from one point to another through a wire. Such phenomenon can be achieved when electron-weak puller metal is connected with electron-strong puller metal through a wire in which electrons move from anodes to cathodes spontaneously [13]. A traditional example of dry battery can be illustrated when zinc metal (weak pull for electrons) and copper (strong pull for electrons) rods are connected to each other through electrolyte. In such a process, one side (zinc) will lose electrons through oxidation reaction at anodes and the other side (copper) will gain electrons through reduction reaction at cathodes. This process is known as galvanic or voltaic cells where chemical reactions, specifically an oxidation/reduction reaction, create electricity [14].

The basic structure of the voltaic cells is illustrated in Fig. 1 in which the main components are represented, and the main idea of moving electrons is clarified [15].

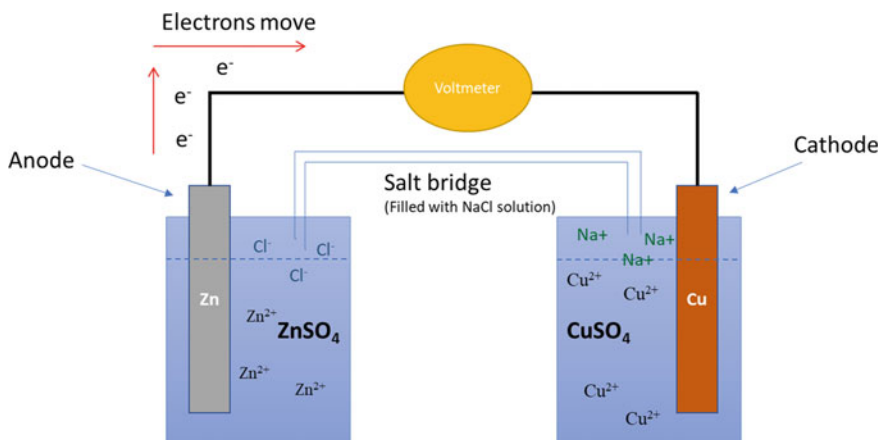


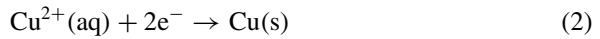
Fig. 1 Voltaic cell

A typical voltaic cell is composed of two half-cells, each half-cell contains a metal that is immersed in a solution [16]. Initially, Zn metal is oxidized by losing electrons that move through a wire to a cathode, made of copper (Cu), resulting in releasing Zn^{2+} ions in the $ZnSO_4$ solution. On the other half-cell, Cu is gaining electrons from the Zn half-cell resulting in converting Cu^{2+} ions in the $CuSO_4$ solution into Cu metal atoms. As a result, Zn rod in the first half-cell dissolves as Zn metal convert to Zn^{2+} ions. However, Cu rod, in the second half-cell, increases in mass as Cu^{2+} ions converts to Cu metal atoms. More importantly, a salt bridge made of NaCl helps to balance these charges that built up in the two half-cells by releasing Na^+ ions in the Cu half-cell and releasing Cl^- ions in the Zn half-cell.

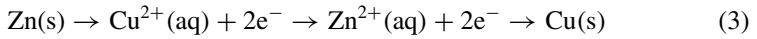
Accordingly, the oxidation reaction can be summarized in the following equation (Eq. 1) in which sold Zn metal losing two electrons, as they move out, to turn to Zn^{2+} ion which is dissolved into the solution of the oxidation half-cell.



The reduction reaction can also be summarized in the following equation (Eq. 2) in which Cu^{2+} ion which is in the solution of the reduction half-cell gains 2 electrons and turns into solid Cu that is attacked by the copper rod (cathode).



Finally, the overall reactions that took place into the two half-cells can be put together in the following equation (Eq. 3):



Based on the reduction potential, E_{red}^0 of the reduction half-cell and the reduction potential of the reverse oxidation half-cell (E_{oxi}^0) as mentioned in Eq. 4, total cell potential can be calculated by the addition of the two half-cells potential. In the case of Zn/Cu dry cells, the an overall cell potential is the sum of $E_{red}^0 = 0.339$ V and $E_{oxi}^0 = 0.762$ V to end up with overall standard cell potential equal to 1.101 V [17].

$$E_{oxi}^0 = -E_{red}^0 \quad (4)$$

The calculation of the overall cell potential is carried out based on the standard reduction potential (Table 1) that occurred in the standard condition state (concentrations 1 mol/L, pressures 1 atm and temperature 25 °C) [18].

If the reduction/oxidation reaction process takes place in an unlike the standard condition, the following equation (Eq. 5) is applied to calculate the standard cell potential:

$$E_{cell} = -E_{cell}^0 - \frac{RT}{nF} \ln Q \quad (5)$$

Table 1 Standard Reduction Potentials

Half reaction	Potential
Pb ⁴⁺	+1.67 V
Cu ²⁺	+0.34 V
Zn ²⁺	-0.76 V
Al ³⁺	-1.66 V
Li ⁺	-3.05

where E_{cell} = The cell potential at non-standard condition; E_{oxi}^0 = cell potential at standard condition; R (gas constant) = $8.314 \text{ J}\cdot\text{K}^{-1}\text{mol}^{-1}$; T = Kelvin temperature; F = Faraday's constant; n = number of moles of electrons; Q = reaction quotient [19].

1.2 Factors Affecting the Cell Potentials and Current Density

In light of oxidation/reduction mechanism, it has been reported many factors that influence the cell electrochemical properties such as the recharging cell mechanism, the cell voltage, and the cell current density [20].

In rechargeable batteries, oxidation/reduction reactions, occurred in the dry cells, have to be reversible in which negative charges are compelled to move toward the anode (in the charging phase) instead of the cathode. For instance, lead–acid battery [21] is one of the most popular rechargeable batteries found in the automobiles which have lead metal as an anode and lead oxide as a cathode [22]. The cell potential of one single lead-acid cell equal to 2.02 V, while a six-pack of lead-acid cells packed together in a parallel position can obtain ~12 V battery [23]. Accordingly, cell potential can be increased by using multiple packs of cells connected in barrel position.

However, the cell current density can be significantly increased by increasing the surface area of anode by using, for instance, electrodes in powder form instead of metal form [24]. Based on this phenomenon, the electrospinning technique has been recently employed to obtain nanofibers as a platform for advanced rechargeable/chargeable batteries in terms of improving the power density and cyclability [25]. Therefore, nanofibers have been immensely involved in secondary battery composition in anodes [26], cathodes [27], separators [28], and as catalytic materials [29], as it will be discussed in the next subsections.

1.3 Basics of Electrospinning Technique

Electrospinning technique has been discovered in the last decades in order to produce fibers in nanoscaled diameter by using high-power supply [30–33]. Basically, the

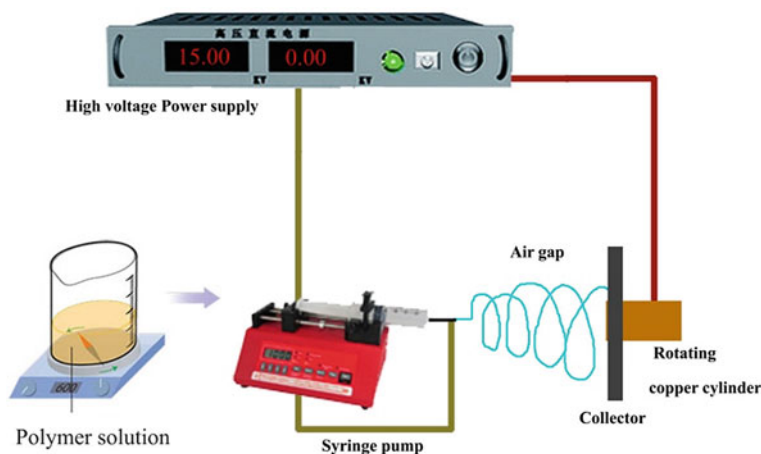


Fig. 2 Basic diagram of the electrospinning apparatus

average of the human hair diameter is 17–171,000 nm, while the average diameter of electrospun fibers can range from few microscales to 30–50 nm or less [34]. Electrospinning technology has several benefits such as high surface area of the electrospun fibers; producing fibers made of unconventional substrates and using dry process with limited hazard solvents [35].

The main components of the electrospinning technique can be summarized as high-power supply (0–60 kV or more); feeding system (syringe pump in nozzle or drum in needleless systems) and receiver plate, drum, or conveyor. Figure 2 shows the basic diagram of the house-made electrospinning apparatus in which single nozzle is used to inject the polymer solution through a syringe needle connected to a high-power supply. The ejected fibers are passing through the airgap in which solvents get evaporated and dry nanofibers are deposited onto a plate receiver.

However, electrospinning apparatus has been developed by replacing the plate collector by drum collector (Fig. 3) with speed controller [36, 37]. Such a drum collector has been used to enhance the fiber alignment and control the fiber diameter [38, 39].

In order to increase the productivity of the electrospun fibers, the single nozzle has been changed to multi-nozzle [40, 41] or shower-like extrusion systems (Fig. 4), and the ejected fiber are received either on drum collectors or conveyors [42, 43]. Recently, needleless electrospinning [44, 45] has been emerged to increase the mass production of nanofibers. In such technique, ground-charged wire is adjustable, in the horizontal direction, to control the airgap distance. The receiving non-woven substrate is fixed on rolling cylinders, in the vertical direction, with a speed controller to adjust the thickness of the electrospun mats (substrate speed range 0–5000 mm/min). Power supply can be monitored and provide a wide range span from 0 to 80 kV. The polymer cartridge boat carries solutions range from 20 mL to 50 mL [46].

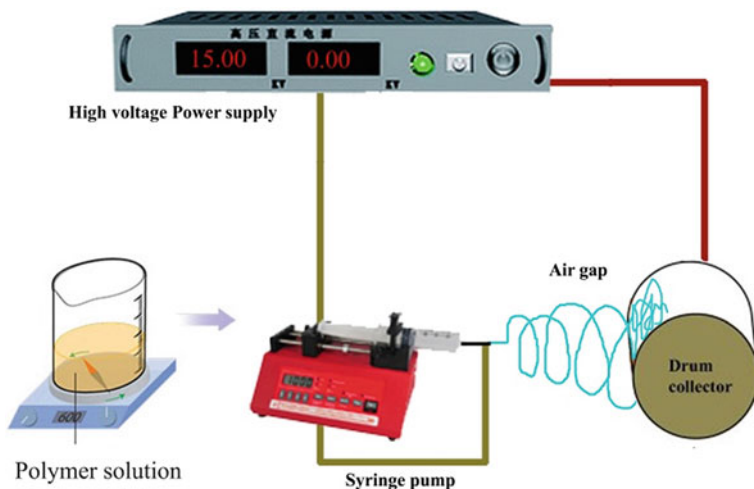


Fig. 3 Advanced electrospinning apparatus with drum collector

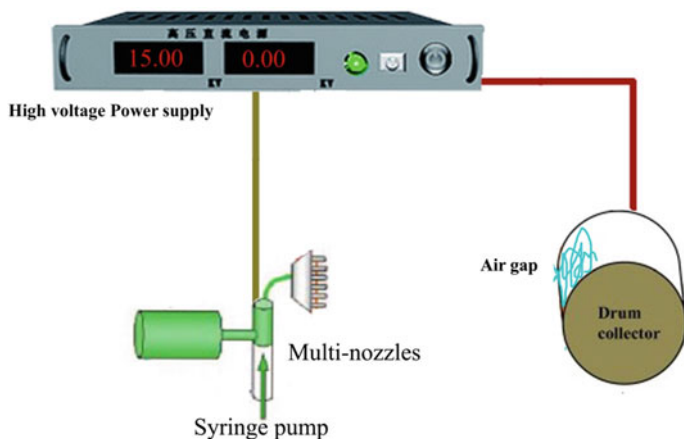


Fig. 4 Multi-nozzle electrospinning apparatus with drum collector

2 Applications of Electrospun Fibers in Batteries

2.1 Electrospun Fibers in Metal–Air Batteries

Principally, metal–air batteries are based on pure metal anodes made of lithium, zinc, or aluminum and external cathode of ambient air with aqueous electrolytes. Typically, as electrons move from anodes during the discharging process, metal anode is getting oxidized. The specific capacity and energy density of such metal–air batteries are

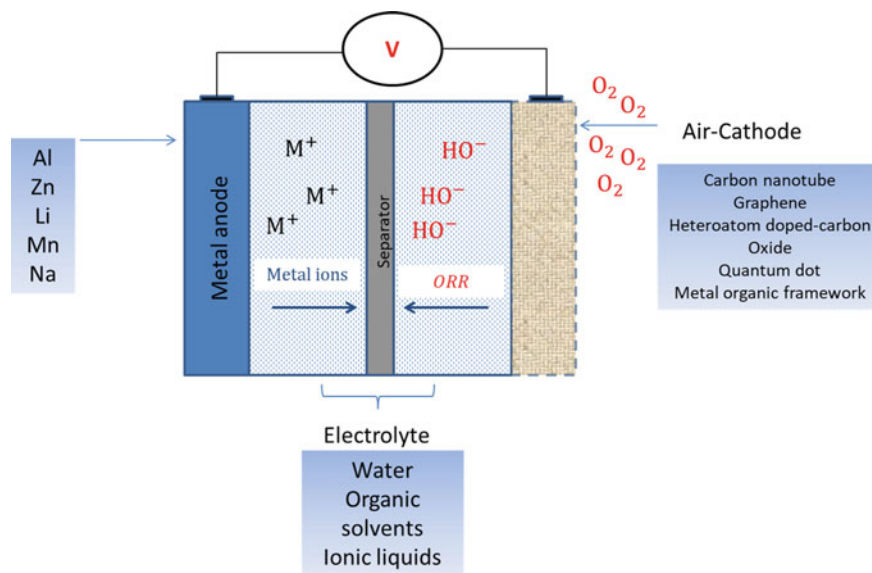


Fig. 5 Schematic diagram of metal–air batteries

much higher than that of metal-ion batteries. For example, lead–acid batteries can produce 30 watt-hours per kilogram (kg) of storage unit, while lithium-ion batteries can produce 100–200 watt-hour per kg of storage unit. However, aluminum–air batteries can produce 8100 watt-hour per kg of storage unit [47].

Typically, the generated electricity in such type of batteries, in discharging process, is carried out by the oxidation reaction of the metal to superoxides or peroxides (Fig. 5) by which electrons move out to the air-cathodes reacting with oxygen to produce water (H_2O) and hydroxides (HO^-) in a process called oxygen reduction reaction (ORR). Metals such as lithium, sodium and potassium which are very sensitive to water, are oxidized in aprotic solvents instead [48].

The reliability of such batteries can be precisely measured by calculating different parameters such as the polarization performance, the round-trip efficiency, and the Coulombic efficiency. The polarization performance can be calculated by measuring the current density at a specific discharge voltage, while round-trip efficiency gives an information about the ratio between the energy released in the discharging process and the required energy in the charging process. The Coulombic efficiency is the most important parameter for rechargeable batteries which is defined as the ratio between the charge capacity and the discharge capacity at full cycle of discharge–charge process. In optimum conditions for batteries, Coulombic efficiency must be %99.98 to show initial capacity higher than 80% after 1000 charging cycles.

Metal–air batteries [49] have some limitations with the irreversible consumption of the metal electrodes resulting in low Coulombic efficiency. Also, the reduction reaction of oxygen in the air-cathode is very sluggish in kinetic. Much has been done

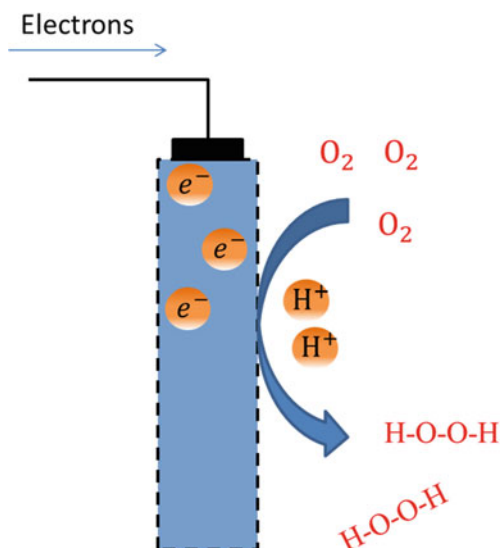
to mitigate such drawbacks and to enhance the life-cycle to metal–air batteries that will be addressed in the following subsections [50].

2.1.1 Electrospun-Based Electro-Catalyst for Metal–Air Batteries

In order to enhance the rechargeability of metal–air batteries, bifunctional catalysts have been used to regulate the reduction reaction of oxygen and lower the overpotentials of the discharging and charging processes. Carbon nanotube-based bifunctional catalysts have been used [51] immensely to accelerate the oxygen reduction reaction (ORR) in the discharging process (Fig. 6) and the oxygen evolution reaction (OER) in the charging process. Heteroatom-doped graphene-based electrocatalysts [52], Perovskite oxides [48], and many others have been used to accelerate the same process. However, other research groups have been worked on changing the surface area of such electrocatalysts by using electrospinning technique to boost their activities. Also, hydrogels [53–55] with high ionic conductivity have been used to enhance the reversibility and stable cycle [56], as flexible supercapacitor electrodes [57] and, gel electrolyte [58].

Xu et al. [59] developed porous Perovskite oxide-based catalyst nanotube by using the electrospinning technique to produce nanofiber forms that were exposed to a calcination process at 650 °C for 3 h. Final porous catalyst showed a significant acceleration to the ORR and OER processes, lower the overpotentials and resulting in improving the round-trip efficiency in lithium–air batteries. Such high catalytic activity of the porous Perovskite-based catalyst showed high specific capacity and

Fig. 6 Oxygen reduction reaction mechanism in the metal–air cathodes



good cycle stability for batteries. Park et al. [60] reported a new class of bifunctional electrocatalyst to ORR and OER based on porous nanorods of $\text{La}_{0.5}\text{Sr}_{0.5}\text{Co}_{0.8}\text{Fe}_{0.2}\text{O}_3$ and reduced graphene oxide/nitrogen-doped. Authors blended the inorganic catalysts with fluoro-based polymer, Nafion, as a carrier to obtain electrospun fibers which was calcinated at $700\text{ }^\circ\text{C}$ for 3 h. Nanoscaled composite was mixed with N-doped reduced graphene oxide to end up with very active bifunctional electrocatalyst for rechargeable metal–air batteries by accelerating ORR and OER in alkaline electrolyte. This is due to the large surface area of the porous structure of the prepared electrocatalyst.

Peng et al. [61] fabricated air-cathode for zinc–air battery by using the coaxial electrospinning technique in different approaches. Author used polyacrylonitrile polymer as a shell layer which impregnated with cobalt acetate tetrahydrate and thiourea. While poly(methyl methacrylate) was used as a core substrate. Mixture was electrospun at 18 kV with shell diameter 750 nm and core diameter 420 nm. After thermal treatments of the electrospun fibers, poly(methyl methacrylate) was vanished to gases and the shell substrate (poly-acrylonitrile) was carbonized via stabilization thermal treatment at $280\text{ }^\circ\text{C}$ for 0.5 h and at $800\text{ }^\circ\text{C}$ for 2 h under argon atmosphere. This process produced hollow fibers made of carbon nanofibers decorated by cobalt/sulfur-doped. Data revealed that the hollow and porous structure of the doping of nitrogen and sulfur showed a better electrical conductivity, bifunctional catalysts, and exhibited preferable performance toward ORR.

2.1.2 Electrospun-Based Composites of Anodes for Metal–Air Batteries

Anodes in metal–air batteries, during the discharging and charging processes, is subjected either to shape change or corrosion especially in alkaline electrolytes which lead to shortening of cycle life [50]. To solve this issue, it has been developed different methods to decrease or prevent the corrosion process during the discharging/charging process. It has been reported that alloying pure metals such as aluminum [62] with different metals such as copper [63], magnesium [64], titanium [65], etc., has shown a significant impact to reduce the corrosion tendency in the alkaline electrolytes. Also, it has been investigated that adding either organic or inorganic additives [66, 67] as inhibitors can reduce the corrosive effect of electrolytes. Recently, coating anode surface by protecting interlayer has been reported to control the anode corrosion. Sol–gel method has been used to fabricate Al_2O_3 thin film on Zn-electrode in order to mitigate the electrode corrosion [68].

Zuo et al. [69] electrospun polyacrylonitrile incorporated with Al_2O_3 , using DMF as a solvent, to achieve a $4\text{ }\mu\text{m}$ electrospun mat on an aluminum foil sheet. Fiber diameters were around 450 nm and thermally stabilized at $300\text{ }^\circ\text{C}$ for 2 h. The produced interlayer helped to suppress the corrosion of the aluminum anode and resulted in a significantly high capacity (1255 mAh/g at 5 mA/cm^2) and a remarkable stability.

2.1.3 Electrospun-Based Composites of Cathodes for Metal–Air Batteries

Metal–air batteries are distinguished by air-cathode in which the main reactant, oxygen, is obtained from air. Therefore, cathode is composed of electrocatalyst (to reduce the electrode overpotential) and a porous layer. The latter layer acts as a gas-diffuser to regulate the oxygen diffusion through the electrocatalyst. The main concern in the air-cathode is the accumulation of reaction products such as Li_2O_2 , and Li_2O , in case of lithium–air batteries, on the cathode. Therefore, air-cathode has to be fabricated of high electroconductive substrates with large surface area and porous structure in order to facilitate the electrons pathways. As a result, the fabrication methods of the air-cathodes have been widely investigated to overcome the above-mentioned issues.

Casting is the most considerable method to fabricate the air-cathode in which conductive paste was cast on conductive metals in a foam form. However, such method leads to side reactions during the discharging and charging processes [15]. Therefore, other routes have been discovered to produce self-standing electrospun composites as air-cathodes.

Song et al. [70] fabricated such self-standing air-cathode based on cobalt ions linked to benzimidazolate ligands that has been blended with carbonization-capable polymers such as polyacrylonitrile. The latter slurry was electrospun followed by two-post thermal treatments to end up with Co_3O_4 /nanotube composites that used as an air-cathode without the need to a binder or metal foam. The results demonstrated much higher discharging capacities (760 mA h/g), lower charging overpotential and enhanced cycle performance.

Nitrogen-doped carbon nanofibers containing iron carbide has been electrospun by Ma et al. group [71] and was utilized as an air-cathode in flexible aluminum–air battery. Authors synthesized Fe_3C nanophases that were encapsulated in nitrogen-doped carbon nanofibers. Typically, polyacrylonitrile polymer was used as a carrier to contain the iron metal-organic frameworks which was electrospun with an average fiber diameter of 300 nm. The produced fibers were exposed to a thermal treatment in nitrogen atmosphere to obtain N-doped porous carbon nanofibers decorated with Fe_3C nanoparticles. This study showed outstanding catalytic activity and stability toward oxygen reduction reaction and showed a stable discharge voltage (1.61 V) for 8 h, giving a capacity of 1287.3 mA h/g.

Bending-resistant cathode for aluminum–air battery has been fabricated based on carbon nanofibers incorporated with magnesium oxide (Mn_3O_4). It has been reported [72] that magnesium oxide was mixed with polyacrylonitrile to be electrospun in single needle at 17 kV. Electrospun fibers, with average fiber diameter of 400 nm, were calcinated at 900 °C for 1 h. Data showed that the fabricated Al–air battery can be discharged over 1.2 V under 2 mA/cm² at dynamic bending state, and a specific capacity up to 1021 mA h/cm².

Bui et al. [73] reported the electrochemical performance of non-woven mats made of carbon nanofibers incorporated with different metals (platinum, cobalt, and

palladium) as air-cathodes for lithium-oxygen battery (in organic solvent as electrolyte). Authors fabricated the air-cathodes by using a typical carbonization-capable polymer, polyacrylonitrile, as a core substrate and poly(vinylpyrrolidone) [46] as a shell substrate. Metal precursors (platinum acetylacetonate, palladium acetate and cobalt acetate tetrahydrate) were added to the core substrate and were electrospun at 12 kV. Electrospun fibers with fiber diameter 720 nm (390 shells and 165 nm core) were subjected to thermal treatments started by stabilization in air at 300 °C for 4 h, and then under nitrogen at 300–750 °C for 1 h and at 750–1200 °C for 2 h. The electrochemical performance of the pure carbon nanofiber cathode was compared with those decorated with the metals. Results stated that the discharge/charge profiles are looked the same. However, the specific capacity of platinum-decorated carbon nanofibers was much higher (5133 mAh/g at 1000 mAh/g) than that of the reference cathode (1533 mAh/g at 1000 mAh/g). Also, data showed overpotentials of both on discharging and charging processes reduced with platinum-decorated carbon nanofibers and remarkably prolonged cycle life (163 cycles).

2.2 Electrospun Fibers in Metal-Ion Batteries

Metal-ion rechargeable batteries are considered as fast-growing technologies for energy storage devices, in the last few decades. This is due to their high density of power and energy associated with long life cycle [74]. Basically, metal-ion cell as a rechargeable cell, metal ions move from negative electrodes to positive electrodes in discharging process and vice versa in charging process. The flow of such ions leads to a flow of electrons that move in a circuit to generate energy. Accordingly, Metal-ion batteries consist of four main components namely: anode, cathode, electrolyte, and separator. The most common metals used in such batteries are aluminum, lithium, sodium, and potassium. In the following subsections, utilization of electrospinning technique in metal-ion batteries will be limited and discussed for lithium-ion batteries as a role model.

2.2.1 Electrospun Materials for Lithium-Ion Batteries

Although lithium-ion batteries have been used globally in different applications, researchers are still urged to develop low cost, high power density, and high energy lithium-ion batteries. Typically, lithium-ion batteries have been made of graphite cathodes and lithium metal-based anodes in the presence of lithium salt mixed in organic solvents [75]. As a result of many incidents regarding to lithium-operated portable devices, lithium oxides and different alloys have been developed to provide safe and reliable lithium batteries. The main measurements used to reflect the batteries' performances are the specific capacity and the operation current densities. These two parameters are determined by the electrochemical performance of the electrode materials used in batteries [76].

Recently, nanostructured electrodes have been utilized to enhance the electrochemical performance in metal-ion batteries. This is due to the tremendous increase in the surface area which leads to a decrease in the mass and charge diffusion, shortens the transporting path of ions, increases the electron transfer, and finally improves the intercalation kinetics [77].

Many different approaches have been tackled to prepare one-dimensional nano-materials for electrodes such as chemical vapor deposition, self-assembly, solvothermal method, solution-growth and electrospinning technique. The latter approach, electrospinning technique, is very simple way to produce one-dimensional nano-sized materials for electrodes with wide diversity in morphological characteristics.

2.2.2 Electrospun-Based Cathodes in Lithium-Ion Batteries

In lithium-ion batteries, much has been studied to improve the energy density and the operating cell voltage. Lithium-based transition metal oxides showed very promising approach to obtain high energy density for such type of batteries. Of these compositions, lithium/iron/phosphate composite has been used due to its thermal stability and large energy density (170 mAh/g). However, this alloy showed lower cell operating voltage (3.5 V). Kang et al. [78] studied the effect of introducing manganese to the previous composite in electrospun fibers. The authors prepared electrospinning solution based on poly(vinyl pyrrolidone) with lithium, manganese, iron, and phosphate salts and ejected it under certain condition for electrospinning. Solutions were electrospun at 10–15 kV with average fiber diameter of 100–500 nm. The electrospun fibers were air-dried at 100 °C, calcinated at 500 °C for 10 h, and then post-calcinated at 800 °C in nitrogen atmosphere. Hagen et al. [79] reported that the cyclic voltammetry analysis showed the cell operating voltage increased from 3.5 to 4.1 V in the presence of manganese element in lithium cathode. Study showed that by increasing the manganese content in the electrospun fibers, cell voltage increased over 4.6 V with maximum discharge capacities 125 mAh/g.

Many different polymers have been used in order to provide self-supporting cathodes made of lithium-based transition metal oxides by utilizing electrospinning technique. Polyacrylonitrile has been used by Toprakci et al. [80] with LiFePO_4 composite to provide carbon nanotube-supported Li-cathode with total high capacity 166 mAh/g.

Lithium vanadium phosphate ($\text{Li}_2\text{V}_2(\text{PO}_4)_3$) composite is another Li-based transition metal oxide that has been addressed in order to obtain better energy density. This cathode composition provides 190 mAh/g capacities with stable three-dimensional framework and poor electrochemical output. To solve this problem, the ionic conductivity has been improved by developing nano-scaled platform of $\text{Li}_3\text{V}_2(\text{PO}_4)_3$. For example, Chen et al. [81] used poly (4-vinyl) pyridine as a carrier, mixed with NH_4VO_3 , $\text{NH}_4\text{H}_2\text{PO}_4$, and citric acid for electrospinning. Mixture has been electrospun at 32 kV to obtain nanofibers with average diameters of 170–440 nm. These fibers have been calcinated at 800 °C for 4 h to retain the fibrous structure with

average diameters 90–220 nm. $\text{Li}_3\text{V}_2(\text{PO}_4)_3$ carbon nanofibers composite exhibited good cycle performance, capability in average voltage 3.0–4.8 V, and high discharge capacity of 190 mAh/g.

Another research group prepared two different layers of LiFePO_4 and $\text{Li}_4\text{Ti}_5\text{O}_{12}$ carbon nanofibers to study the electrochemical performance [82]. Different metal salts were mixed with polyacrylonitrile and polyvinylpyrrolidone, electrospun at 25 kV, pre-oxidized at 260 °C for 2 h and then calcinated at 800 °C for 10 h in N_2 atmosphere. The two-layer cathode showed very promising capacity in terms of charged/discharged processes up to 800 cycles at 1C with a retention capacity of more than 100 mAh/g and a Coulombic efficiency close to 100%.

2.2.3 Electrospun-Based Anodes in Lithium-Ion Batteries

Anodes for lithium-ion batteries have a great impact on the overall performance in terms of charge/discharge rate capability, cyclability, and energy storage capacities. Developed anodes for Li-ion batteries showed several principles that have to be addressed such as cost and environmental concerns, hosting large numbers of Li-ions during the charging process, made of materials that are insoluble in the electrolyte solvents, and have a reduction potential as high as lithium metal (–3.05 V).

Over the past decade, graphite has been chosen as a promising candidate for lithium-ion anodes due to its abundance, reversibility with high Coulombic efficiency, and energy capacities (372 mAh/g). However, towards electric car applications require long cell lifetime and cell operating voltage, there are many challenges to anode materials that have to be addressed in the fabrication process. Again, nanostructured anodes have been an approach to solve the problem addressed above. This hypothesis has been firstly approved, in 1996, when Liu et al. [83] prepared hard carbon samples from calcinated epoxy resins with nanoporosity. Study proved that large specific capacity for lithium was recorded as a function of the number of single carbon layers in the heat-treated epoxides. Since then, increasing the surface area of electrodes is an approach to enhance the lithium-ion batteries.

Electrospinning technique was one of these approaches to fabricate Li-ion anode with very high surface area which is capable of hosting many lithium ions during the charging process. Kumbar et al. [84] prepared carbon nanotube using a typical procedure of the electrospinning of polyacrylonitrile followed by a calcination step in inert atmosphere (N_2) at 800 °C. Polyacrylonitrile was electrospun at 21 kV with gap distance 14 cm to obtain fibers with average diameters 200 nm. The electrochemical lithium storage properties showed discharge capacities of 826 and 370 mAh/g for the first and second cycles respectively, at a current density of 200 mA/g with capacity 200 cycles.

Kim et al. [85] used 10% of polyacrylonitrile in dimethylformamide and electrospun the solution using 25 kV. Polyacrylonitrile electrospun fibers were obtained with average diameter 200–300 nm, thermally treated at 280 °C for 1 h and then calcinated at three different temperatures 700, 1000 and 2800 °C under inert atmosphere (argon). Data showed that the best results were recorded to the nanofibers

that calcinated at 1000 °C to give a large reversibility of 450 mAh/g and high rate capability 100 mAh/g.

Other elements have been addressed to improve the graphite capacity (372 mAh/g) such as incorporating tin, tin oxide, and tin composites. Theoretical capacity of tin is 993 mAh/g and when it mixed with graphite anodes enhances the overall capacities. However, because its expansion during charge/discharge process, it cracks and results in rapid fading to the cell capacity. Nanostructured tin or tin alloy in different shapes such as nanoparticles, thin films and nano-wire have been reported to solve this problem. For this purpose, Zou et al. [86] prepared tin/carbon non-woven film via electrospinning technique. Author used polyvinyl alcohol (PVA), 10% wt/v of 80,000 MW, mixed with 10% wt/v of tin(II) chloride and 20% v/v distilled water. Solution was electrospun at 25 kV, air-gap distance (15 cm) and flow rate (1 mL/h). Electrospun fibers with tin nanoparticles in 0.33 nm was dedicated by high resolution transmission electron microscope (HRTEM) and was heated at 500 °C in argon/ H₂ atmosphere for 3 h. The electrochemical investigation of the non-woven film showed a reversible capacity after 20 cycle of a 382 mAh/g which is 96% of the capacity in the first cycle.

Nickel oxide is another element that showed a significant interest to enhance the lithium-ion batteries owing to its high theoretical capacity (718 mAh/g). However, in bulk form, nickel oxide showed very poor electrochemical performance due to its large volume change during charge/discharge process and low electronic conductivity. Porous nickel oxide anodes with nano-morphologies such as nano-sheet, nano-wall, and nano-spheres have been considered to improve the electrochemical properties. Wang et al. [87] prepared lithium-ion anode based on carbon nanofibers incorporated with nickel oxide. Authors used polyacrylonitrile (10% wt/v) mixed with nickel nitrate salt for electrospinning at 10 kV, air-gap distance 15 cm and flow rate 0.9 mL/h. Nanoweb was thermally treated at 300 °C for 1 h and at 600 °C for 5 h and then at 350 °C for 2 h in inert atmosphere (N₂). The porous anodes including nickel oxides showed high reversible capacity of 638 mAh/g over 50 cycles.

Another super promising candidate, silicon, has been reported for lithium-ion batteries owing to its very high gravimetric specific capacity (4200 mAh/g). Like other elements, silicone has four times volume expansion during charge/discharge process resulting in rapid fading of the battery capacity. Silicon nanoparticles (50 nm) have been mixed [88], in different ratios, with 7.5% wt/v solution of polyacrylonitrile (MW 86,000) in dimethylformamide to obtain electrospun composites. This nanoweb composite was pre-oxidized in air for 6 h at 240 °C to protect the fibrous morphology during following carbonization steps. Post-thermal treatment at 600 °C in inert atmosphere (argon) was conducted to the nanoweb composites for 8 h. At ratio C/Si (77/23 wt/wt), silicon composite carbon nanofibers showed a large reversible capacity up to 1240 mAh/g.

Agglomeration of silicone nanoparticles has been an issue to obtain well distributed electrospun precursor solutions for electrospinning. Xu et al. [89] worked on de-agglomeration of silicon nanoparticles by conducting different treatments in order to obtain well-dispersed solution for electrospinning. Silicon nanoparticles (50–100 nm) were initially stirred magnetically in piranha solution (H₂SO₄/H₂O₂=7:3

v/v) for 2 h at 80 °C, centrifuged in deionized (DI) water and diluted into 200 mL ethanol solution to obtain hydroxyl-terminated silicon. The latter was treated via 3-aminopropyl trimethoxysilane to obtain the amino-silane functionalized silicon nanoparticles. The modified silicon nanoparticles were mixed with 7% wt/v polyvinyl alcohol (MW 86000–124000) which is more compatible with the functionalized silicon nanoparticles. Nanoweb was stabilized at 200 °C for 2 h and then at 650 °C for 1 h in inert atmosphere (nitrogen gas). The obtained electrode exhibited an excellent electrochemical performance with a discharge capacity of 872 mAh/g (after 50 cycles) and capacity retention of 91%.

In the light of the above mentioned modifications, silicon nanoparticles had to be treated through sophisticated processes and hazard materials in order to provide well distributed nanoparticles. Therefore, it has been a challenge to find out an ecofriendly alternative to synthesis carbon-based composites with good electrochemical properties.

Cobalt oxide has been an example for experimental trials to obtain carbon-based electrode with large reversible capacity, excellent cyclic performance, and good rate capacity. Zhang et al. [90] prepared cobalt oxide-based carbon nanofibers via the electrospinning of polyacrylonitrile, Mw 150000, mixed with Cobalt acetate tetrahydrate. After thermal treatment at 650 °C for 2 h in nitrogen gas, data showed that cobalt compound was CoO rather than Co or Co₃O₄. The obtained cobalt-based electrode showed a good electrochemical performance of 633mAh/g after 52 cycles.

2.2.4 Electrospun-Based Separators and Electrolytes in Lithium-Ion Batteries

As described before, electricity is produced from lithium batteries as electrons move in a wire and lithium ions move in the electrolyte between cathodes and anodes back and forth during the charge/discharge process. Accordingly, electrolyte with very high ionic conductivity is highly demanded to the lithium-ion batteries as long as it meets the environmental, safety, and cost concerns. It has been using the organic solvents in such lithium-ion batteries until concerns about flammability, explosion, and volatilization have been raised [91].

On the other side, separators have very crucial role in secondary batteries and especially in lithium-ion batteries to ensure the safety of the batteries by preventing the direct contact between anodes and cathodes and allow ion transfer through microscopic holes. Accordingly, separators must satisfy all the physical and electrochemical conditions.

Much has been investigated that solid polymer electrolytes can be employed in lithium-ion batteries as electrolyte and separator, in the same time, provided to meet the basic requirements of the electrochemical conductivity and the chemical, thermal and mechanical stability [92]. In the very beginning, polyethylene oxide (PEO) has been investigated as a promising candidate to provide thinner and safer lithium-ion batteries. Different drawbacks in PEO that have been reported constrain its applications in lithium-ion batteries. PEO high crystallinity especially at room temperature

leads to a huge constraint in the ionic conductivity. The deterioration in PEO mechanical strength at higher temperatures is another reason. These limitations of solid polymer electrolytes remain as main challenges to upscale the battery production.

Therefore, much has been done in this field to enhance the PEO crystallinity by different means such as chemical modifications, blending with other polymers, and mixing with conductive additives [91]. In this part, fabrication of such polymer solid electrolytes via electrospinning will be the main concern.

Samad et al. [93] investigated the effect of blending PEO solutions with a novel cellulosic reinforcement material, named GELPEO, on the mechanical properties of PEO electrospun fibers as solid polymer electrolyte. Author electrospun 10% wt/v of PEO ($M_w = 300,000$) associated with different concentrations of GELPEO (5, 10 and 20 wt/v) at 20 kV, flow rate 1 mL/h and the electrospun fibers were received on rotating drum at 200 rpm. Data showed that tensile strength values have improved by two-fold and the composite fibers are thermally stabilized up to 200 °C. Unlike the expected, addition of 5% wt/v of GELPEO did not show significant reduction in the ionic conductivity and gives very comparable measurements (4×10^{-4} S/cm) compared to PEO fibers (5×10^{-4} S/cm).

Another research group from Iran [94] studied the effect of ZnO and TiO₂ nanoparticles embedded on electrospun fibers of PEO associated with lithium perchlorate. Fibers were electrospun at 18.4 kV, flow rate 0.5 mL/h, distance 15 cm and fibers were collected on rotating drum at 100 rpm. Authors used a potentiostat/galvanostat instrument to evaluate the cycling stability of PEO with/without ZnO and TiO₂ nanoparticles. Data showed that highest values of the ion conductivities were recorded for of 0.21 wt% of the TiO₂ and ZnO to reach 0.045 mS/cm and 0.035 mS/cm, respectively. These values were considered much higher than that of the same composition used for casting thin films which recorded 0.0044 mS/cm and 0.0147 mS/cm for TiO₂ and ZnO respectively. However, it has been reported that such filler-filled electrospun solid electrolyte loss up to 40% of its capacity after 45 cycles.

The same research group [95] investigated the effect of ethylene and propylene carbonates (EC and PC), as plasticizers to the PEO electrospun fibers, on the electrolyte electrochemical performance. Authors recorded the highest value in ionic conductivity, at ratio 3:1 (EC:PC), 0.171 mS/cm. More PC to the PEO resulted in decreasing the cycle capacity significantly.

Zhu et al. [96] studied the effect of adding high ionic conductive ($\text{Li}_{0.33}\text{La}_{0.55}\text{TiO}_3$) nanowires to PEO electrospun fibers on the electrochemical properties of the final solid composite electrolyte. The ionic conductive nanowire was prepared by the electrospinning of PVP solutions mixed with lithium salt (LiNO_3), lanthanum salt ($\text{La}(\text{NO}_3)_3$) and Ti (OC_4H_9)₄, dissolved in DMF solutions and followed by thermal treatments. Authors obtained nanofibers of PEO incorporated with the ($\text{Li}_{0.33}\text{La}_{0.55}\text{TiO}_3$) nanowires along with propylene carbonate, plasticizer, as a solid composite electrolyte. Data showed that by adding 8% of the nanowires to PEO, the ionic conductivity of the composite has reached to the maximum value at 5.66×10^{-5} and 4.72×10^{-4} at 0 °C and 60 °C, respectively. The obtained composite electrolyte exhibited an initial reversible discharge capacity of 135 mAh/g and good cycling stability.

Poly(vinylidene fluoride), PVdF has been used as solid polymer electrolyte in lithium batteries due to its high mechanical stability, its polar nature owing to the fluorine atoms, and for being chemically inert. However, PVdF showed a low ionic conductivity owing to its crystallinity which leads to migration hindrance of lithium ions.

Gopalan et al. [97] prepared electrospun solid polymer electrolyte based on PVdF mixed with different amounts of poly(diphenylamine), PDPA (0.5, 1 and 2% w/w). Mixture was electrospun at 25 kV, 10 mL/h flow rate and 15 cm distance to obtain electrospun fibers with average diameter 200 nm. The final electrolyte composite of PVdF/PDPA electrospun fibers were soaked in a mixture of lithium salts (lithium perchlorate) and propylene carbonate. Electrochemical properties showed superior activity in terms of ionic conductivity, electrochemical stability and good interfacial behavior with electrode.

The same research group investigated the electrochemical properties of the composition of PVdF with polyacrylonitrile (PAN) prepared via electrospinning [98]. Mixture of PVdF and different proportions of PAN were dissolved in DMF:acetone (7:3 v/v) and electrospun at 25 kV, 10 mL/h flow rate, 20 cm distance and fibers were received on rotating drum. The electrolyte composite was obtained by soaking the electrospun mat in a mixture of lithium salts (lithium perchlorate) and propylene carbonate. PVdF/PAN composite electrolyte, prepared by 25% PAN, showed a high amount of lithium salt uptake of the electrolyte (300%) and a high ionic conductivity of 7.8 mS/cm.

The copolymer of PVdF with hexafluoropropylene (HFP) has been reported as a good solid polymer electrolyte owing to its good electrochemical stability and affinity to electrolyte solutions. Li et al. [99] reported the electrochemical properties of PVdF-co-HFP electrospun membrane. Polymer ($M_w = 4.77 \times 10^5$) at a concentration of 12–18 wt/v, dissolved in acetone/dimethylacetamide (7/3, wt/wt) was electrospun at 18 kV to obtain fibers of average diameter 1 μm . The electrolyte was prepared when PVdF-co-HFP was soaked in lithium salts/propylene carbonate solutions. The solid copolymer (PVdF-co-HFP) electrolyte showed a high electrolyte uptake and ionic conductivities of 10^{-3} S/cm.

Other research groups investigated the influence of the incorporation of ceramic fillers on the ionic conductivity of the solid polymer/composite electrolytes. Raghavan et al. [97] reported the electrochemical performance of the electrospun composite of PVdF-co-hexafluoropropylene and silica. The copolymer was mixed with in-situ prepared silica and ball mill prepared silica and their electrochemical characteristics were compared to PVdF-co-hexafluoropropylene fibers. Electrospun solutions were obtained at 20 kV, 0.1 mL/min flow rate, 16 cm distance, and received on rotating drum at 140 rpm. Obtained electrospun fibers were investigated on scan electron microscope (SEM) to show an average diameter of 1–2 μm . The final composite electrolytes were prepared by immobilizing lithium salt (lithium hexafluorophosphate) and ethylene carbonate/dimethyl carbonate in the electrospun mats. In general, the prepared composites exhibited high electrolyte uptake (550–600%), while the superior electrochemical performance recorded for the polymer electrolyte containing 6% in situ silica with ionic conductivity of 8.06 mS/cm at 20 °C.

Cui et al. [100] investigated more complicated approach by preparing solid composite electrolyte when PVdF was mixed with modified titanium dioxide (TiO_2). Initially, aminated TiO_2 was grafted by poly(methyl methacrylate) via atom transfer radical polymerization technique. The grafted TiO_2 was mixed with PVdF before electrospinning. Fibers were electrospun at 14 kV and 20 cm distance. Electrospun fibers of PVdF/grafted TiO_2 with an average diameter 0.333–0.336 μm were soaked in lithium salt (1 M of lithium hexafluorophosphate) in ethylene carbonate/DMF. Data showed that the presence of grafted TiO_2 inhibits the crystallization of PVdF in the solidification process and enhances the ionic conductivity of the final solid composite electrolyte. The improved electrochemical performance was recorded for the composite electrolyte containing 6% wt (based on the weight of PVdF) grafted TiO_2 and showed ionic conductivity of 2.95 mS/cm at 20 °C compared to 2.51 mS/cm of PVdF electrolyte.

Thermoplastic polyurethane (TPU) electrospun fibers have been employed as mold for solid composite electrolyte when it soaked in fillers to enhance the ionic conductivity. In 2018, Gao et al. [101] electrospun 17% wt/v of TPU at 20 kV, at 40 °C and used rotating drum as a collector. The obtained mat was soaked in PEO solution containing nano-sized SiO_2 and lithium bis(trifluoromethanesulfonyl)imide (LiTFSI)salt. Data revealed that the final composite electrolyte of TPU-PEO with 5 wt% SiO_2 and 20 wt% LiTFSI showed an ionic conductivity of 6.1×10^{-4} S/cm at 60 °C with a high mechanical stability of 25.6 MPa. Battery made of this solid composite electrolyte and LiFePO_4 cathode showed a discharge capacity of 152, 150, 121, 75, 55 and 26 mA h/g at C-rates of 0.2C, 0.5C, 1C, 2C, 3C and 5C, respectively. The discharge capacity of this lithium-ion battery remains 110 mA h/g after 100 cycles at 1C at 60 °C with capacity retention of 91%.

However, Zainab et al. [102] used the electrospun fibers of polyurethane mixed with polyacrylonitrile to build up a composite used as separator in lithium-ion batteries. Fibers were obtained using electrospinning technique at 25 kV, at flow rate 1 mL/h, 15 cm distance and collected on rotating drum at 50 rpm. Data revealed that ionic conductivity has improved up to 2.07 S/cm, with high mechanical stability up to 10.38 MPa and good anodic stability up to 5.10 V were observed. The thermal stability of PU/PAN separator displayed only a 4% dimensional change after 0.5 h of long exposure at 170 °C.

Different combinations of several conductive polymers have been utilized as solid composite electrolyte for lithium-ion batteries. Peng et al. [103] obtained new electrospun electrolyte made of TPU and PVdF-*co*-HFP dissolved in DMF/acetone (1:1 wt/wt) and electrospun at 24.5 kV. The vacuum-dried electrospun mat was soaked in 1 M of lithium perchlorate/ethylene carbonate. Data showed that the ionic conductivity value has enhanced up to 6.62×10^{-3} S/cm. Composite showed very decent value of tensile strength (9.8 ± 0.2 MPa) and elongation at break ($121.5 \pm 0.2\%$). Battery, made of this composite electrolyte and Li/PE/LiFePO_4 cathode, provides a high initial discharge capacity of 163.49 mAh/g under 0.1 C rate.

Tan et al. [104] fabricated electrospun fibers made of a mixture of three polymers PAN, TPU and polystyrene (PS) in mass ratio 5:5:1. The three polymers were dissolved under vigorous stirring in DMF for 12 h at 60 °C before the spinning step.

Electrospun fibers of PAN/TPU/PS were obtained at 24 kV and extruded at flow rate 0.5 mL/h. The composite electrolyte was obtained by soaking these electrospun fibers in 1 M of a solution of lithium hexafluorophosphate/ethylene carbonate. The prepared solid composite electrolyte showed an ionic conductivity of $3.9 \times 10 \text{ mS/cm}$ at room temperature and an electrochemical stability of 5.8 V. However, battery made of this composite electrolyte and LiFePO_4 cathode, exhibited charge and discharge capacities of 161.70 mAh/g and 161.44 mAh/g, respectively, at a 0.1 C rate. Battery showed a stable cycle performance in the capacity retention of 94% after 50 cycles and high Coulombic efficiency.

Other research group investigated more complicated composites to provide better ionic conductivity, thermal and mechanical stabilities. Yang et al. [104] prepared solid composite electrolyte based on electrospun filaments and silicon-based conductive additive. The silicon-based additive was synthesized by refluxing γ -chloropropoyl trimethoxy silane in acid/anhydrous ethanol medium at 40 °C for 5 days. The dry substance was mixed, in different concentrations, to PVdF/PAN/PMMA polymers in solid ratio (2:2:1). The polymer solution (15% wt/v) was electrospun at 20 kV, flow rate 1.8 mL/h, air-gap distance 25 cm and fibers were collected on rotating drum at 50 rpm. Data showed that the average diameter of PVdF/PAN/PMMA electrospun fibers was 600 nm and with silicon-additive 2, 4, 6, 8, 10 and 12%wt/v diameters have increased to 740, 770, 820, 810, and 800 nm, respectively. The electrochemical characteristics of the composite electrolyte of 10 wt% silicon-additive exhibited a high electrolyte uptake of 660% and an excellent thermal stability. Also, the solid composite electrolyte showed ionic conductivity potent of 9.23 mS/cm at room temperature and electrochemical stability is up to 5.82 V.

Maurya et al. [105] prepared solid composite electrolyte based on electrospun membrane and hetero-nano particles of rare-earth elements. Different concentrations of lithium, lanthanum, barium, and zirconium salts were mixed together in the presence of citric acid at 120 °C until milky powder was obtained. Different concentrations of the calcinated powder (5, 10 and 15% wt/v) were added to a solution of PVdF-co-HFP (16% wt/v) dissolved in a mixture of solvents (dimethylacetamide and acetone 3:7). Solutions were electrospun at 18 kV, 12 cm distance and a flow rate of 0.5 mL/h. The obtained membranes were dried on vacuum at 60 °C, pressed to 25–45 μm thickness and soaked in 1 M of a liquid electrolyte of lithium hexafluorophosphate in ethylene carbonate/dimethyl carbonate. Data showed that the ionic conductivity has improved to 3.30 mS/cm at 25 °C with a working potential of 4.6 V. Battery assembled from this composite exhibited a superior specific capacitance of 123 F/g at a current density of 1 A/g with a capacity retention of 83% even after 1000 cycles.

Other research group used electrospinning technique to prepare sandwich-like composite electrolyte via layer by layer technique of different polymers. Qin et al. prepared a sandwich-like structure made of two layers of PVdF-co-HFP and a polyamide-6 layer in between. Electrospinning conditions were optimized to fabricate bead-free and uniform electrospun fibers. Both fibers were layer-by-layer received on the same target to produce the final membrane. The composite electrolyte

was prepared by soaking the prepared sandwich-like membrane in lithium hexafluorophosphate. Sandwich mat picked up 270% of the liquid electrolyte and showed acceptable mechanical properties up to 17.11 megapascal. The composite electrolyte showed a high ionic conductivity of 4.2 mS/cm at room temperature and stable electrochemical window of a 4.8 V. In the assembled battery of this composite electrolyte and lithium anode and lithium iron phosphate cathode, high electrochemical stability, high discharge capacity and good cycle durability were observed.

3 Conclusion and Outlook

Rechargeable batteries hold a prestigious position in the map of the energy-storage research in order to decrease the usage of fossil fuel and decrease the emission of CO₂. Increasing the surface area of the main components of batteries showed a significant increase in the electrochemical performance of such batteries. The electrospinning technique, to fabricate nano-sized fibers, can be utilized in coating, decorating, or constructing the cell components which is considered as a turning point to overcome the drawbacks of the traditional way of fabrications.

Cathodes made of decorated carbon nanofibers with inorganic metals have been emerged recently to enhance the battery density and capacity. Electrospinning techniques can provide different shapes of electrospun fibers in which inorganic nanoparticles can be introduced either in the core or in the shell of carbon nanofibers. Calcinated electrospun fibers can enhance the specific capacity on metal–air battery as much as 5133 mAh/g at 1000 cycles compared to 1533 mAh/g at 1000 cycle of reference cathodes. Generally, electrospun fibers are made of carbonizable polymers that are capable to be carbonized by thermal treatments to provide carbon nanofibers or nanotubes. Such polymers usually have been mixed with many electroconductive enhancers made of nanoparticles of inorganic metals, heteroatom-doped metals, etc. Impregnated polymers have been electrospun either in form of single filaments, core/shell structures, or hollow fibers. Electrospun carbon nanofibers or nanotubes have very large surface area that facilitates the ionic transfer in much higher magnitude compared to regular composites.

Coating of the anode surface by protecting interlayer of electrospun fibers has been reported to control the anode corrosion and to provide high capacity and a remarkable stability.

Electrospun fibers have been used to fabricate solid composite electrolyte by which many drawbacks of liquid electrolyte have been covered. Such composites are made of the electrospun fibers of different polymers that showed good ionic conductivity and high liquid uptake. Such composites showed high mechanical stability and less liquid leakage.

For further development on the utilization of electrospun components in batteries, here are some personal perspectives.

- Utilization of new electrospinning apparatus that provides different fiber orientation and alignment has to be immensely investigated. Fiber direction may have a great impact on the electro-conductivity and the performance of the conversion processes from chemical energy to electric energy and vice versa.
- Synthesis of more carbonization-capable polymers possesses different functional groups may alter the final performance of nanofibers in the voltaic cells.
- The exposure of the electrospun fibers to plasma chamber in the presence of activated different gasses such as nitrogen, argon, fluorocarbon may lead to functionalized electrospun fibers resulting in more porous structure and more surface area.
- More studies are required to enhance the anode corrosion using the electrospun fibers in respect of the adhesion parameter of the electrospun fibers onto the anode surface.
- Monitoring the diameter of the electrospun fibers needs more focus to show the correlation between the fiber diameter and the battery performance.
- More integrated studies to enhance anodes, electrolytes and cathodes may show significant enhancement in the overall performance of batteries.
- Rechargeability is still behind any expectation for batteries and more research is required to enhance it.

Acknowledgements This work was performed during the implementation of the project Building-up Centre for advanced materials application of the Slovak Academy of Sciences, ITMS project code 313021T081 supported by the Integrated Infrastructure Operational Program funded by the ERDF. Author thanks the editor for the kind invitation.

References

1. Sarkar J, Bhattacharyya S (2012) Arch Thermodyn 33:23
2. Poizot P, Dolhem F (2011) Energy Environ Sci 4:2003
3. Kumar Y, Ringenberg J, Depuru SS, Devabhaktuni VK, Lee JW, Nikolaidis E, Andersen B, Afjeh A (2016) Renew Sustain Energy Rev 53:209
4. Aziz MS, Ahmed S, Saleem U, Mufti GM (2017) Int J Renew Energy Res 7:111
5. Jia T, Dai Y, Wang R (2018) Renew Sustain Energy Rev 88:278
6. Giwa A, Alabi A, Yusuf A, Olukan T (2017) Renew Sustain Energy Rev 69:620
7. Rosa AP, Chermicharo CAL, Lobato LCS, Silva RV, Padilha RF, Borges JM (2018) Renew Energy 124:21
8. Alexander S, Harris P, McCabe BK (2019) J Clean Prod 215:1025
9. Kuncoro CBD, Luo WJ, Kuan Y Der (2020) Int J Energy Res 1
10. Shepherd CM (1965) J Electrochem Soc 112:657
11. Patrício J, Kalmykova Y, Berg PEO, Rosado L, Åberg H (2015) Waste Manag 39:236
12. Tar B, Fayed A (2016) IEEE 59th Int Midwest Symp Circuits Syst (IEEE), pp 1–4
13. Weppner W (2000) Mater. Lithium-Ion Batter. (Springer Netherlands), pp 401–412
14. Qu D (2014) AIP Conf Proc, pp 14–25
15. Li M, Li YT, Li DW, Long YT (2012) Anal Chim Acta 734:31
16. Jorňe J, Kim JT, Kralik D (1979) J Appl Electrochem 9:573
17. Sapkota P, Kim H (2009) J Ind Eng Chem 15:445

18. Koebel M (1974) *Anal Chem* 46:1559
19. Titi ST (1986) *Pure Appl Chem* 58:955
20. Tarhan L, Acar B (2007) *Res Sci Technol Educ* 25:351
21. Ballantyne AD, Hallett JP, Riley DJ, Shah N, Payne DJ (2018) *R Soc Open Sci* 5
22. Manwell JF, McGowan JG (1993) *Sol Energy* 50:399
23. Burzyński D, Kasprzyk L (2017) *E3S Web Conf* 14
24. Deng T, Lu Y, Zhang W, Sui M, Shi X, Wang D, Zheng W (2018) *Adv Energy Mater* 8
25. Jing M, Zhang X, Fan X, Zhao L, Liu J, Yan C (2016) *Electrochim Acta* 215:57
26. Li L, Ding Y, Yu D, Li L, Ramakrishna S, Peng S (2019) *J Alloys Compd* 777:1286
27. Singh A, Kalra V (2019) *J Mater Chem A* 7:11613
28. Wang L, Wang Z, Sun Y, Liang X, Xiang H (2019) *J Memb Sci* 572:512
29. Ma W, Xu Y, Ma K, Zhang H (2016) *Appl Catal A Gen* 526:147
30. Subbiah T, Bhat GS, Tock RW, Parameswaran S, Ramkumar SS (2004)
31. Frey MW (2008) *Polym Rev* 48:378
32. Bhattarai P (2014) Thapa KB, Sharma S, Basnet RB, p 3809
33. Yong K, Jeong L, Ok Y, Jin S, Ho W (2009) *Adv Drug Deliv Rev* 61:1020
34. Schiffman JD, Schauer CL (2008) *Polym Rev* 48:317
35. Kessick R, Fenn J, Tepper G (2004) *Polymer (Guildf)* 45:2981
36. Nada AA, Ali EA, Soliman AAF, Shen J, Abou-Zeid NY, Hudson SM (2020) *Int J Biol Macromol*
37. Al-Moghazy M, Mahmoud M, Nada AA (2020) *Int J Biol Macromol* 160:264
38. Katta P, Alessandro M, Ramsier RD, Chase GG (2004) *Nano Lett* 4:2215
39. Haider S, Al-Zeghayer Y, Ahmed Ali FA, Haider A, Mahmood A, Al-Masry WA, Imran M, Aijaz MO (2013) *J Polym Res* 20
40. Lee EJ, An AK, Hadi P, Lee S, Woo YC, Shon HK (2017) *J Memb Sci* 524:712
41. Kim IG, Lee JH, Unnithan AR, Park CH, Kim CS (2015) *J Ind Eng Chem* 31:251
42. Dos Santos AM, Dierck J, Troch M, Podevijn M, Schacht E (2011) *Macromol Mater Eng* 296:637
43. Wang S, Yang Y, Zhang Y, Fei X, Zhou C, Zhang Y, Li Y, Yang Q, Song Y (2014) *J Appl Polym Sci* 131:2
44. Yang Z, Peng H, Wang W, Liu T (2010) *J Appl Polym Sci* 116:2658
45. Yarin AL, Zussman E (2004) *Polymer (Guildf)* 45:2977
46. Zahran SME, Abdel-Halim AH, Mansour K, Nada AA (2020) *Int J Biol Macromol* 157:530
47. Qin J, Liu Z, Wu D, Yang J (2020) *Appl Catal B Environ* 278:
48. Han S, Hao Y, Guo Z, Yu D, Huang H, Hu F, Li L, Chen HY, Peng S (2020) *Chem Eng J* 401
49. Zhao H, Yuan ZY (2021) *J Energy Chem* 54:89
50. Wang HF, Xu Q (2019) *Matter* 1:565
51. Chen Z, Yu A, Higgins D, Li H, Wang H, Chen Z (2012) *Nano Lett* 12:1946
52. Li JC, Hou PX, Liu C (2017) *Small* 13:1
53. Ragab TIM, Nada AA, Ali EA, Shalaby ASG, Soliman AAF, Emam M, El Raey MA (2019) *Int J Biol Macromol* 135:407
54. Nada AA, Ali EA, Soliman AAF (2019) *Int J Biol Macromol* 131:624
55. Nada AA, Soliman AAF, Aly AA, Abou-Okeil A (2018) *Starch Stärke* 71:1800243
56. Han Q, Chi X, Zhang S, Liu Y, Zhou B, Yang J, Liu Y (2018) *J Mater Chem A* 6:23046
57. Shi Y, Pan L, Liu B, Wang Y, Cui Y, Bao Z, Yu G (2014) *J Mater Chem A* 2:6086
58. Wang SH, Hou SS, Kuo PL, Teng H (2013) *ACS Appl Mater Interfaces* 5:8477
59. Xu JJ, Xu D, Wang ZL, Wang HG, Zhang LL, Zhang XB (2013) *Angew Chemie Int Ed* 52:3887
60. Park HW, Lee DU, Zamani P, Seo MH, Nazar LF, Chen Z (2014) *Nano Energy* 10:192
61. Peng W, Wang Y, Yang X, Mao L, Jin J, Yang S, Fu K, Li G (2020) *Appl Catal B Environ* 268:
62. Birbilis N, Buchheit RG (2005) *J Electrochem Soc* 152:B140

63. Kowal K (1996) *J Electrochem Soc* 143:2471
64. Song G (2005) *Adv Eng Mater* 7:563
65. Wolfe RC, Shaw BA (2007) *J Alloys Compd* 437:157
66. Ibrahim NA, Nada AA, Hassabo AG, Eid BM, Noor El-Deen AM, Abou-Zeid NY (2017) *Chem Pap* 71:1365
67. Eid BM, Hassabo AG, Nada AA, Ibrahim NA, Abou-Zeid NY, Al-Moghazy M (2018) *Adv Nat Sci Nanosci Nanotechnol* 9:
68. Wongrujipairoj K, Poolnapol L, Arpornwichanop A, Suren S, Kheawhom S (2017) *Phys Status Solidi Basic Res* 254
69. Zuo Y, Yu Y, Liu H, Gu Z, Cao Q, Zuo C (2020) *Batteries* 6:1
70. Song MJ, Kim IT, Kim YB, Shin MW (2015) *Electrochim Acta* 182:289
71. Ma Y, Sunboja A, Zang W, Yin S, Wang S, Pennycook SJ, Kou Z, Liu Z, Li X, Wang J (2019) *ACS Appl Mater Interfaces* 11:1988
72. Yu Y, Zuo Y, Liu Y, Wu Y, Zhang Z, Cao Q, Zuo C (2020) *Nanomaterials* 10
73. Bui HT, Kim DY, Kim DW, Suk J, Kang Y (2018) *Carbon N Y* 130:94
74. Robert Ilango P, Peng S (2019) *Curr Opin Electrochem* 18:106
75. Kalluri S, Seng KH, Guo Z, Liu HK, Dou SX (2013) *RSC Adv* 3:25576
76. Li W, Zeng L, Wu Y, Yu Y (2016) *Sci China Mater* 59:287
77. Liu D, Cao G (2010) *Energy Environ Sci* 3:1218
78. Kang CS, Kim C, Kim JE, Lim JH, Son JT (2013) *J Phys Chem Solids* 74:536
79. Von Hagen R, Lorrmann H, Möller KC, Mathur S (2012) *Adv Energy Mater* 2:553
80. Toprakci O, Ji L, Lin Z, Toprakci HAK, Zhang X (2011) *J Power Sources* 196:7692
81. Chen Q, Zhang T, Qiao X, Li D, Yang J (2013) *J Power Sources* 234:197
82. Chen LL, Yang H, Jing MX, Han C, Chen F, Hu X yu, Yuan WY, Yao SS, Shen XQ (2019) *Beilstein J. Nanotechnol* 10:2229
83. Liu Y, Xue JS, Zheng T, Dahn JR (1996) *Carbon NY* 34:193
84. Suresh Kumar P, Sahay R, Aravindan V, Sundaramurthy J, Ling WC, Thavasi V, Mhaisalkar SG, Madhavi S, Ramakrishna S (2012) *J Phys D Appl Phys* 45:
85. Kim C, Yang KS, Kojima M, Yoshida K, Kim YJ, Kim YA, Endo M (2006) *Adv Funct Mater* 16:2393
86. Zou L, Gan L, Kang F, Wang M, Shen W, Huang Z (2010) *J Power Sources* 195:1216
87. Wang B, Cheng JL, Wu YP, Wang D, He DN (2012) *Electrochem Commun* 23:5
88. Wang L, Ding CX, Zhang LC, Xu HW, Zhang DW, Cheng T, Chen CH (2010) *J Power Sources* 195:5052
89. Xu ZL, Zhang B, Kim JK (2014) *Nano Energy* 6:27
90. Zhang M, Uchaker E, Hu S, Zhang Q, Wang T, Cao G, Li J (2013) *Nanoscale* 5:12342
91. Li L, Peng S, Lee JKY, Ji D, Srinivasan M, Ramakrishna S (2017) *Nano Energy* 39:111
92. Xue Z, He D, Xie X (2015) *J Mater Chem A* 3:19218
93. Samad YA, Asghar A, Hashaikeh R (2013) *Renew Energy* 56:90
94. Banitaba SN, Semnani D, Heydari-Soureshjani E, Rezaei B, Ensafi AA (2019), *Mater. Res. Express* 6
95. Banitaba SN, Semnani D, Heydari-Soureshjani E, Rezaei B, Ensafi AA (2020) *Solid State Ionics* 347
96. Zhu L, Zhu P, Yao S, Shen X, Tu F (2019) *Int J Energy Res* 43:4854
97. Gopalan AI, Lee KP, Manesh KM, Santhosh P (2008) *J Memb Sci* 318:422
98. Gopalan AI, Santhosh P, Manesh KM, Nho JH, Kim SH, Hwang CG, Lee KP (2008) *J Memb Sci* 325:683
99. Li X, Cheruvally G, Kim JK, Choi JW, Ahn JH, Kim KW, Ahn HJ (2007) *J Power Sources* 167:491
100. Cui WW, Tang DY, Gong ZL (2013) *J Power Sources* 223:206
101. Gao M, Wang C, Zhu L, Cheng Q, Xu X, Xu G, Huang Y, Bao J (2019) *Polym Int* 68:473
102. Zainab G, Wang X, Yu J, Zhai Y, Ahmed Babar A, Xiao K, Ding B (2016) *Mater Chem Phys* 182:308

103. Peng X, Zhou L, Jing B, Cao Q, Wang X, Tang X, Zeng J (2016) *J Solid State Electrochem* 20:255
104. Tan L, Deng Y, Cao Q (2019) *Jing B. Liu Y, Wang X*, p 3673
105. Maurya DK, Murugadoss V, Angaiah S (2019) *J Phys Chem C* 123:30145